of the values given by Hays[6] ($\langle a^2\rangle = 0.033$) from an analysis of microwave-absorption measurements on Zn.

V. CONCLUSIONS

Although the absolute precision of the pure-Zn parameters reported here is restricted by the Mn corrections, the uncertainties associated with previously reported values have been reduced. The individual quantities T_0, H_0, γ, and $(dH_c/dT)_{T=T_0}$ measured herein all fall within the range of previously reported values. An examination of these previously reported values shows that low values of T_0 correspond to low values of H_0, and both are probably due to magnetic impurities.

The determination of $\langle a^2\rangle$ to be 0.03 ± 0.005 by means of Eq. (7) is only slightly affected by the Mn impurities. The effects of magnetic impurities are such that they would tend to give an overestimate of $\langle a^2\rangle$ rather than an underestimate.[17] It is felt therefore that the value of $\langle a^2\rangle = 0.035$ which was obtained from the uncorrected data (see Fig. 3) represents an upper limit to the $\langle a^2\rangle$ determination and is so indicated by the error limits imposed on the best estimate of $\langle a^2\rangle$ which is 0.031.

[1]N. E. Phillips, Phys. Rev. Lett. **1**, 363 (1958).
[2]G. Seidel and P. H. Keesom, Phys. Rev. **112**, 1083 (1958).
[3]R. E. Fassnscht and J. R. Dillinger, Phys. Rev. **164**, 565 (1967).
[4]F. W. Smith, J. Low Temp. Phys. **5**, 683 (1971).
[5]D. Farrell, J. G. Park, and B. R. Coles, Phys. Rev. Lett. **13**, 328 (1964).
[6]D. A. Hays, Phys. Rev. B **1**, 3631 (1970).
[7]D. U. Gubser and L. D. Jones, Rev. Sci. Instrum. **43**, 943 (1972).
[8]D. U. Gubser and D. E. Mapother, Rev. Sci. Instrum. **40**, 843 (1969).
[9]R. A. Hein and R. L. Falge, Jr., Phys. Rev. **123**, 407 (1961).
[10]G. Boato, G. Gallinaro, and C. Rizzuto, Phys. Rev. **148**, 353 (1966).
[11]D. Markowitz and L. P. Kadanoff, Phys. Rev. **131**, 563 (1963).
[12]J. R. Clem, Phys. Rev. **153**, 449 (1967).
[13]J. R. Clem, Ann. Phys. (N.Y.) **40**, 268 (1966).
[14]This value is the average of those values reported in Refs. 4 and 10.
[15]Authors are grateful to D. Farrell for the use of this sample which was prepared by him.
[16]D. U. Gubser, Phys. Rev. B **6**, 827 (1972).
[17]W. R. Decker and D. K. Finnemore, Phys. Rev. **172**, 430 (1968).

PHYSICAL REVIEW B VOLUME 7, NUMBER 9 1 MAY 1973

Anomalous Ultrasonic Attenuation in Pure Superconducting Nb†

Frank Carsey*
National Oceanics and Atmospherics Administration, Wave Propagation Laboratory, Boulder, Colorado 80302 and Department of Physics, University of California, Los Angeles, California 90024

Moisés Levy
Department of Physics, University of Wisconsin-Milwaukee, Milwaukee, Wisconsin 53201 and Department of Physics, University of California, Los Angeles, California 90024

(Received 19 June 1972)

Pure-state data are presented for ultrasonic attenuation in clean Nb (resistivity ratio ≈ 7000) in the domain $0.4 < ql < 6$, where $q = 2\pi/\lambda$ is the phonon wave vector for phonons of wavelength λ and l is the electronic mean free path. These results are presented in light of the models of Fate and Trivisonno, Lacy and Daniel, and Maki. In general, no model is found completely adequate.

INTRODUCTION

The ultrasonic measurement[1-7] of the superconducting energy gap of pure superconductors has long differed both from the idealized models[8-12] and from other energy-gap measurements such as tunneling.[13-15] Most recently niobium of extremely high purity has become available, primarily through Dr. R. E. Reed of the Oak Ridge Laboratories, permitting measurements on samples characterized by phonon-limited mean free paths. In this case the ultrasonic attenuation for phonons with $ql < 1$ shows marked deviation[16-18] from that expected by simple models. In this paper we briefly summarize the models presented thus far, along with their domains of "good" fit. In addition we present shear and longitudinal-attenuation data on high-purity niobium in the normal and superconducting states. Where it is possible these data are compared with available theory. Our data fall in the region $0.4 < ql < 6$, where $q = 2\pi/\lambda$ is the phonon wave vector for phonon of wavelength λ and l

is the electronic mean free path.

The first model proposed to account for the attenuation for long-mean-free-path superconductors was that of Maki[1,19–22] who used the Green's functions of Eliashberg.[23] Maki accounts for deviation of the data from BCS-like behavior by taking into account the increased absorption of phonons by electrons of energy near the edge of the gap. This increase in absorption is due to the singularity in the density of (final) states near the edge of the energy gap compared to the density of states for the normal state. Thus the electron-phonon portion of the mean free path is decreased in the superconducting state. This model provides a deviation from BCS which increases with increasing temperature since the contribution of the electron-phonon portion of the mean free path compared to the impurity-scattering portion increases as the temperature increases. Specifically Maki finds that the mean free path is energy dependent and given by

$$l(\omega)=\left(l_0^{-1}+\frac{|\omega|}{(\omega^2-\Delta^2)^{1/2}}\,\Theta(|\omega|-\Delta)\,BT^3\right)^{-1}$$

for the superconducting state and $l_n=(l_0^{-1}+BT^3)^{-1}$ for the normal state. In the above ω represents the electronic energy, l_0 is the zero-temperature mean free path, $\Theta(x)$ is zero for $x\leq 0$ and equal to 1 otherwise, and $B\cong 1.2/\mathrm{K}^3\,\mathrm{cm}^{-1}$ is considered a constant for niobium independent of purity. If the energy gap is assumed to be BCS like, Maki predicts two limiting values. $\Delta_{\mathrm{BCS}}(0)$ is the zero-temperature gap parameter at low temperatures ($t=T/T_c<0.4$), and $\Delta_{\mathrm{ap}}(0)$ is the zero-temperature gap parameter for $t\lesssim 1$. The ratio of these energy gaps is expressed[1] as a function of purity $\Delta_{\mathrm{ap}}(0)/\Delta_{\mathrm{BCS}}(0)=f(x)$; $x=l_0BT_c^3$, where $1\leq f(x)\leq\frac{1}{2}\pi$ for $0\leq x<\infty$.

Trivisonno[5] *et al.* modify the model of Fate[6] *et al.* (hereinafter FT) which employs a mean-free-path influence on the ratio α_s/α_n for $ql<1$ where the electronic mean free path is not impurity limited. In their view $\alpha_s/\alpha_n=[Q(ql_s)/Q(ql_n)]2F$, where $F=(e^{\Delta/kt}+1)^{-1}$ is the BCS distribution function and $Q(ql)$ is the Pippard formula[24] for normal-state attenuation. For $ql<1$ this reduces to $\alpha_s(T)/\alpha_n(T)=(l_s/l_n)\,2F$. This result is usually the next to the last step in deriving the BCS result,[8,10] where the mean free paths are then cancelled due to presumed equality. Since the normalized attenuation falls faster below T_c than the BCS result $\alpha_s/\alpha_n=2F$ predicts, the ratio $l_s/l_n<1$ is in agreement with the result of Maki. There is no technique suggested by FT for evaluating l_s/l_n except as a best-fit procedure. Hence there is no firm temperature dependence implied for l_s/l_n, and some difficulty is experienced in comparing this model with experiments due to the large number of parameters which must be fit. This much is clear in the model of Maki and the model of FT: The temperature dependence of the actual ratio α_s/α_n differs most from the temperature dependence of BCS near the transition. At lower temperatures the attenuation is BCS-like, implying that l_s and l_n have the same temperature dependence. For t near unity the temperature dependence of the ratio is quite substantial indicating that a simple model for l_s is impractical. For small t the normal-state electronic mean free path changes little and the ratio α_s/α_n is BCS-like, leaving the conclusion that for small t l_s and l_n have the same weak temperature dependence, which is to be expected since they are impurity limited.

The most recent model for the normalized ultrasonic attenuation in pure niobium is that of Lacy and Daniel[16] (hereinafter LD) after the theoretical work of Garland.[25] Here one considers the different energy gaps and (possibly) different transition temperatures characteristic of the s-band and d-band electrons.[26] For impure samples the electrons interact so strongly with the lattice that both bands contribute equally and have the same energy gap. With increasing purity the interband-coupling term g_{sd} is sufficiently weak that the superconducting energy gaps are estimated to approach the ratio $\Delta_d/\Delta_s=10$ while retaining $T_c^s=T_c^d=9.24$ K. Hafstrom[27,28] *et al.* after Suhl, Matthias, and Walker[29] visualize a second gap with temperature dependence varying with purity between two limits. The upper limit of $\Delta_s(T)$ is the case of $\Delta_d(T)/\Delta_s(T)=\text{const}$, and the interband coupling is moderately strong. The lower limit is the intraband limit where $g_{sd}=0$. Here $\Delta_s\ll\Delta_d$ and $T_c^s\ll T_c^d$. Intermediate between these two is the weak-intraband–moderate-interband case where $\Delta_d(t)/\Delta_s(t)=\text{const}$ at lower temperatures; here Δ_s does not vanish at a lower T_c^s, but takes an undefined path to become zero at T_c^d. In the latter case the s-band gap parameter $\Delta_s(T)$ is thought to be much smaller than it would be if $\Delta_d(T)/\Delta_s(T)=\text{const}$.

Specifically Lacy and Daniel[16] construct a normalized attenuation which is a weighted sum

$$\frac{\alpha_s}{\alpha_n}=F_1(T)\,\frac{2}{e^{\Delta_1/kT}+1}+[1-F_1(T)]\,\frac{2}{e^{\Delta_2/kT}+1}$$

and choose

$$F_1(T)=\frac{\Delta_1(T)}{\Delta_1(T)+\Delta_2(T)}+\text{const}$$

and

$$\Delta_i(T)=\Delta_i(0)\,\frac{\Delta_{\mathrm{BCS}}(T)}{1.74kT_c}\,.$$

Lacy and Daniel show that this model provides excellent fit to data taken near the transition although it is difficult to judge the quality of the fit

over the entire region $0 < t < 1$ from the comparison given.[16] A weakness of this model may be that the weighting is taken to be independent of temperature. In addition, this model, as it stands, leaves no room for the regularly observed frequency dependence of α_s/α_n.

Thus there are three models for the ultrasonic attenuation ratio α_s/α_n for pure niobium. The model of Maki takes into account an exact dependence of the attenuation on the reduced electronic mean free path in the superconducting state. Fate and Trivisonno modify the BCS equation by multiplying the attenuation ratio by an empirically obtained mean-free-path ratio. Lacy and Daniel pass over mean-free-path considerations to focus on the effects of multiple electron bands in attenuation. Of the three the theory of Maki is based on first principles and leaves no after-the-fact parameters, the model of Fate and Trivisonno contains frequency dependence and the model of Lacy and Daniel takes into account the two-band nature of niobium. A vigorous development of the two-band model attenuation has been undertaken by I-Ming Tang[30] for the mixed state, but thus far there is no continuation of this work for zero-field state.

EXPERIMENTAL RESULTS

Ultrasonic attenuation measurements were made using the standard pulse-echo technique employing the Matec ultrasonic attenuation measuring system. The sample was mounted in a low-pressure chamber immersed in liquid helium which was maintained at $T = 1.4$ K during the course of all experiments. A 15-MHz (fundamental) quartz crystal was bonded to one of two cylindrical niobium samples oriented along the [100] axis. These samples were cut from Oak Ridge Niobium No. 68 and were found to have a resistivity ratio of 7000. Sample data is summarized in Table I. At all times, save during the few minutes required to bond transducer to sample, the samples were stored in liquid nitrogen. The bond used was the standard "dried" and pressed Nonaq bond.[17] In the course of a "run" the sample was heated by being in good thermal contact with a copper block which was in good thermal contact with a resistance-wire heater. The ambient pressure in the space between the sample and the vacuum case was found to lend considerable error to temperature measurement unless it was kept between 2 and 5 Torr. Temperature was measured by comparing the voltage generated across the "voltage" junctions of a Cryocal Cryoresistor (No. 1313) to the voltage dropped across a standard resistor by the same current. The temperature measurements are considered to be accurate to ± 2% with about 0.2% precision. The attenuation measurements accuracy depended on the total attenuation, being about 1% for the first 10 dB, 3% for the second 10 dB, and 5% for the third 10 dB. This error is due to operating out of the linear regions of the logarithmic amplifier.

NORMAL-STATE ATTENUATION

In order to form the ratio α_s/α_n, the normal-state attenuation α_n was measured in zero field and in $H > H_{c2}(0)$. The zero-field data were taken for $T_c < T < 35$ K and the high-field data were taken for $1.3 < T < 35$ K. Following the approach of Tsuda and Suzuki[6] the high-field data were compared to the zero-field data after correcting linearly for the effect of the field:

$$\alpha_n = \alpha_n(\text{measured})\ (\alpha H + \beta).$$

The factor α corrects for shortening of the effective electronic mean free path due to Landau-like orbiting and the factor β is usually viewed as a correction for drift in the attenuation measuring

TABLE I. Niobium sample data: $\alpha_{300\,K}/\rho_{4.2\,K} = 7000$; Orientation, [100]; Length (cm) = 0.853 (Nb No. 11), 0.498 (Nb No. 14); $T_c(H=0) = 9.24 \pm 0.02$ K; $H_{c2}(0) = 3992 \pm 20$ G $\varkappa_{\text{normal}} = 3.8$; $f(\varkappa)_{\text{normal}} = 1.56$.

Phonon	Longitudinal				Shear		
Frequency[a]	15	45	75	105	15	45	MHz
$T=0$; $\alpha_n - \alpha_s$	0.287	0.953	1.85	3.03	1.35	6.74	cm^{-1}
$l(0)$ Temperature dependence	32×10^{-4}	44×10^{-4}	44×10^{-4}	44×10^{-4}	30×10^{-4}	40×10^{-4}	cm
$l(0)$ Frequency dependence	33×10^{-4}	20.4×10^{-4}	38×10^{-4}	30.2×10^{-4}	30×10^{-4}	40×10^{-4}	cm
B	1.32	1.29	1.42	1.27	0.95	0.634	$cm^{-1}\ K^{-3}$
$\Delta_{BCS}(0)/kT_c$	1.74 ± 0.4	1.72 ± 0.02	1.72 ± 0.02	1.78 ± 0.02	1.45 ± 0.1	1.93 ± 0.03	
$\Delta_{ap}(0)/kT_c$	4.05 ± 0.15	3.74 ± 0.12	3.75 ± 0.14	3.52 ± 0.1	5.20 ± 0.15	3.78 ± 0.1	
$f(\varkappa)_{sc} = \Delta_{ap}(0)/\Delta_{BCS}(0)$	2.33 ± 0.1	2.17 ± 0.03	2.16 ± 0.03	1.98 ± 0.02	3.59 ± 0.15	1.96 ± 0.03	

[a]Rounded to nearest harmonic of 15-MHz transducer.

system. α and β are evaluated to make $\alpha_n(H=0)$ exactly agree with $\alpha_n[H>H_{c2}(0)]$ at $T=T_c$. The zero-attenuation calibration point for $\alpha_n(H=0)$ is found by extrapolating the superconducting attenuation down to $T=0$ K for the same run.

α_n measurements were made for several odd-harmonic frequencies of the transducer over the temperature range of interest. The data are compared firstly with the free-electron model of Pippard and others[24] which gives the frequency and mean-free-path dependence of α, and secondly with the same free-electron model but only considering its mean-free-path dependence and suppressing the frequency dependence. In the free-electron model we have chosen $l=(l_0^{-1}+BT^3)^{-1}$, where $l_0=40\times10^{-4}$ cm and $B=1.2$ cm^{-1}K^{-3}, $m^*=m=9.11\times10^{-28}$ g, [31] $v_L=5.41\times10^5$ cm sec^{-1}, and $N=7.84\times10^{22}$. The formulas are

$$\alpha_n^L=\frac{mNv_0\omega}{2\rho_0 v_L^2}\left(\frac{ql\tan^{-1}ql}{3(ql-\tan^{-1}ql)}-\frac{1}{ql}\right)$$

for longitudinal waves and

$$\alpha_n^t=\frac{mNv_0}{\rho_0 v_t l}\left(\frac{1-g}{g}\right),$$

where

$$g=\frac{3}{2ql}\left[\frac{[(ql)^2+1]\tan^{-1}ql}{ql}-1\right],$$

for transverse waves. As before $q=2\pi/\lambda$ is the phonon wave vector for phonons of wavelength λ, v_L and v_t are the sound propagation velocities, v_0 is the Fermi velocity, and ρ_0 is the density. Figure 1 shows the experimentally determined α_n in comparison with the two models. For comparison the data for $T>T_c$ is differentiated according to whether the sample was in zero field or high field. This agreement is excellent. Here the values $\alpha_n[H>H_c(0)]$ have been corrected as described above. The dashed line in Fig. 1 is the predicted attenuation from the free-electron model. These curves have been drawn from parameters evaluated for 15-MHz data. The measured attenuation is progressively larger than the predicted attenuation for larger frequencies. This type of deviation from the free-electron case has been noted in rhenium[32] which is electronically somewhat similar to niobium[31] and in copper[33] and aluminum[34] (which are not). The solid lines are drawn from the free-electron model where the parameter N has been allowed to vary freely. This approach implies that the free-electron model is acceptable except that the entire Fermi-surface electronic population is not allowed to interact with the applied phonons. In reality a deformation-type correction is more justifiable. Our purpose in the construction of the fits shown in the solid lines in Fig. 1 is simply to obtain a functional form for $\alpha_n(T)$ usable in forming the ratio α_s/α_n. These data as well as those for shear waves shown in Fig. 2 have very low-attenuation limits for high T as shown in the graphs. In these data a constant background attenuation has

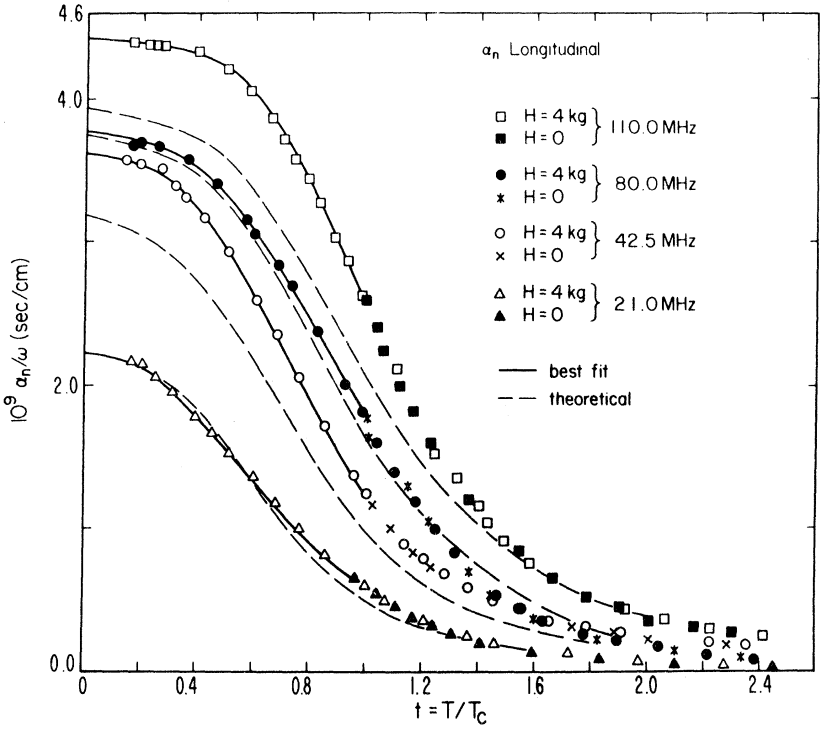

FIG. 1. Normal state longitudinal data vs temperature. Data taken in high field is corrected for magnetic field depression of the attenuation. Both sets of lines are drawn for an electronic mean free path proportional to T^3. The broken lines represent the Pippard free-electron model.

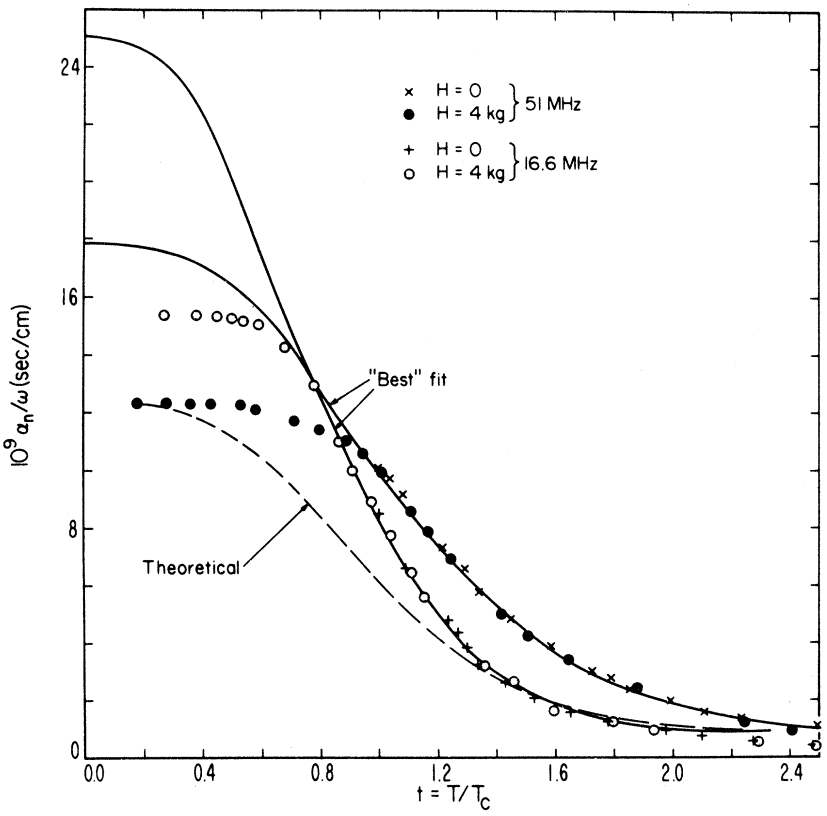

FIG. 2. Normal-state shear data vs temperature. Data taken for $H > H_{c2}(0)$ is corrected for magnetic field depression for the points $t > 1$. The departure of the best-fit curve from the data for $t > 0.8$ is thought to be due to magnetic field effects.

been subtracted. Figure 2 shows similar data and theory for shear waves. Once again points are shown for both zero-field and high-field attenuation where the high-field attenuation has been "corrected." The dashed line is the free-electron model with the parameter N fit at $T = 0$ K for 16.6-MHz phonons. The solid lines are free-electron model functions independently fit to each run for $t > 0.8$. The domain $0 < t < 0.8$ is characterized by having the experimental points well below the "best-fit" lines. The failure of the high-field data for $t < 0.8$ to lie on the expected curve is attributed to magnetic field effects. Earlier work of Levy[35] *et al.* comparing transverse and longitudinal attenuation along the [110] direction on dirtier samples has shown that the ratio $\alpha_n^t(T=0)/\alpha_n^L(T=0)$ is higher than the expected value of 5.38 by about 30%.

Unexplained and heretofore unreported magnetic field effects were observed for shear waves in the experimental geometry $\vec{q} \perp \vec{H}$. Figure 3 shows shear data at 15 MHz taken at $T = 1.5$ K in various fields [all greater than $H_{c2}(0)$]. The solid line is a theoretical conjecture for the qualitative behavior of the electromagnetic portion of the attenuation.[36] The electromagnetic contribution to the attenuation is caused by the production of a net current by the field produced when ionic motion is imperfectly followed by the motion of the electron cloud. This current subsequently suffers resistive-type losses. For $ql > 1$ the electrons responsible for this type of attenuation occupy a limited portion of the Fermi surface. This portion is characterized by containing electrons traveling such that their

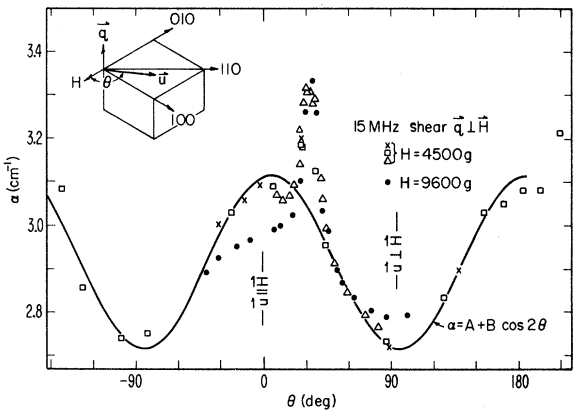

FIG. 3. Shear data in the normal state at $t = 0.16$ for various values of magnetic field as a function of the angle between $\vec{u}$ and $\vec{H}$. The orientation of $\vec{u}$ in the crystal lattice is fixed. The solid line represents a simple model for the behavior of $\alpha_n(0)$. The inset is a schematic showing the orientation of $\vec{q}$, $\vec{u}$, and $\vec{H}$ with respect to the crystal lattice and defines $\theta(\vec{u}, \vec{H})$.

velocity component in the direction of propagation is equal to the sound-wave velocity. Essentially these electrons are those having $\vec{v}_0 \perp \vec{q}$, where $\vec{v}_0$ is the Fermi velocity. In addition, electrons having $\vec{v}_0 \perp \vec{u}$, where $\vec{u}$ is the acoustic translation vector will be accelerated in a direction perpendicular to their motion without a change in energy and hence, for a spherical Fermi surface, into free-electron states of nearly the same energy. These electrons will still reside on the equilibrium Fermi surface and will not have many lower energy states to scatter resistively back into. On the other hand, electrons with $\vec{v}_0 \parallel \vec{u}$ are pushed by the shear phonon perturbation into energies radially displaced (in momentum space) and these electrons will relax into the equilibrium Fermi surface from these new states. Hence more of the attenuation will be due to electrons having $\vec{v}_0 \parallel \vec{u}$. Applying a magnetic field to the sample such that $\vec{q} \perp \vec{H}$ will affect this type of attenuation depending on the angle $\theta = (\vec{u}, \vec{H})$. This is because the mean free path of the attenuating electrons is unaffected when $\vec{H} \parallel \vec{u}$ since then $\vec{H} \parallel \vec{v}_0$ for these electrons and there is no interaction between a moving charge and a magnetic field parallel to it. On the other hand, when $\vec{H} \perp \vec{u}$ then $\vec{H} \perp \vec{v}_0$ and the attenuating electrons are moving at right angles to the field and are accelerated and hence moved prematurely out of the attenuating region of the Fermi surface. It is worth noting that this $(\vec{u} \perp \vec{H})$ is the case at all times when $\vec{q} \parallel \vec{H}$. These arguments lead to the modification of the attenuation for shear waves of $\vec{q} \perp \vec{H}$ by predicting "ripple" proportional to $\cos 2\theta$, or an attenuation depression when $\vec{q} \parallel \vec{H}$. The ripple is represented by the solid line of Fig. 8.

The sharp peak of attenuation for $28° < \theta < 40°$ and correspondingly at $-140° < \theta < -150°$ is without explanation. The [100] crystal orientation along which $\vec{q}$ is directed defines a plane with fourfold symmetry. Any phenomenon characteristic of the Fermi surface[37] for $\vec{H}$ along the [110] direction (as shown in Fig. 3) should appear for H at every [110] axis. This would require four peaks as opposed to the two in the displacement vector $\vec{u}$. This suggests that some quality of the Fermi surface was probed by the attenuating electrons when $\vec{u}$ was more nearly parallel to $\vec{H}$ than when $\vec{u}$ was more nearly perpendicular to $\vec{H}$. These questions lead to further work in this area.

SUPERCONDUCTING-STATE ATTENUATION

Superconducting-state data were taken for shear and longitudinal phonons in the same fashion as normal-state data except that the domains $1.3 < T < 2.5$ K and $9 < T < 9.24$ K were inspected in greater detail and at very slow temperature-drift rate. The data were analyzed in three stages: First the ratio α_s/α_n was formed employing the "best-fit" function $\alpha_n(T)$ described above; secondly the effective BCS energy gap was formed for each value of α_s by inverting the BCS equation $\alpha_s/\alpha_n = 2F(\Delta)$; and thirdly the implied zero-temperature energy gap $\Delta(0)$ was calculated. This last is simply the zero-temperature gap parameter of a BCS-type gap which would have the value $\Delta(T)$ (or $\alpha_s/\alpha_n[T]$) which was measured. In practice the parameter $\Delta(0)$ is found by inverting the expansion of Ferrell[38] $|\Delta(t)/\Delta(0)|^2 = 3.016(1-t) - 2.4(1-t)^2$, where $t = T/T_c$.

Figure 4 shows that temperature dependence of the ratio α_s/α_n for longitudinal and shear attenuation data. The dependence predicted by BCS for a gap of $\Delta(0) = 1.90kT_c$ is also shown. For this curve $\Delta(t) = 1.90\Delta_{BCS}(t)/1.74kT_c$. Both longitudinal and shear attenuation display the frequency dependence previously observed[2-6] and just apparent in the data

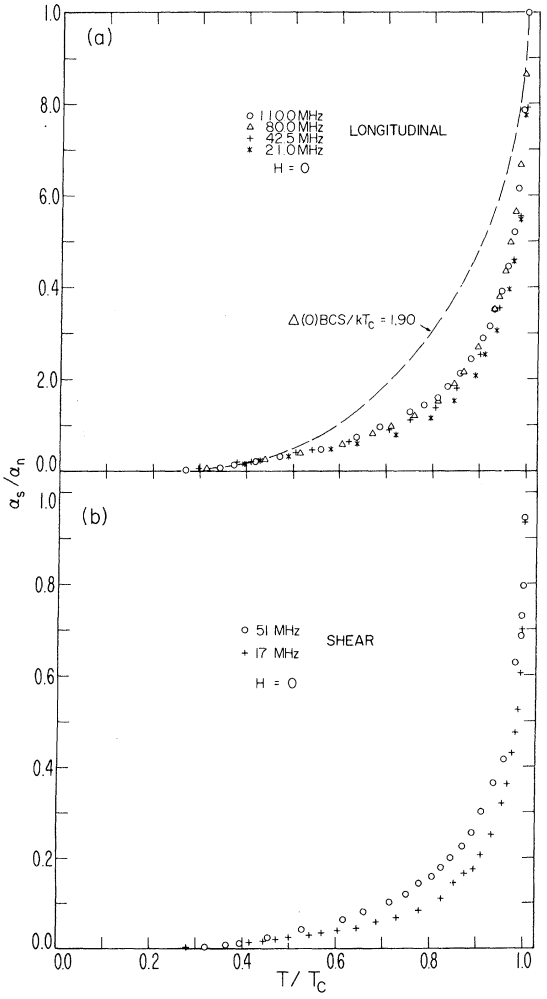

FIG. 4. Temperature dependence of α_s/α_n for longitudinal (a) and shear (b) waves at different frequencies. The broken line is taken from BCS weak coupling limit for $\Delta(0) = 1.90kT_c$.

(Fig. 3) of Ref. 16; the lower-frequency data fall off faster below T_c. We avoid using α_s/α_n curves as a comparison with the models mentioned above because the interesting regions at low and high temperatures are characterized by attenuation data which are essentially asymptotic.

Figure 5 shows longitudinal superconducting state data. Figure 5(a) is a plot of the effective gap obtained by solving the BCS equation for the energy gap $\Delta = t\ln(2\alpha_n/\alpha_s - 1)$ and plugging in values for t and α_s/α_n. The solid line is taken from the model of Lacy and Daniel. Here we have plotted $\Delta/kT_c = t\ln(2/\alpha^* - 1)$, where

$$\alpha^* = \frac{A_1}{A_1+A_2}\left(\frac{2}{e^{\Delta_1/kT_c}+1} + \frac{2}{e^{\Delta_2/kT_c}+1}\right),$$

and

$$\Delta_i = \frac{A_i kT_c}{1.74kT_c}\,\Delta(t),$$

where $\Delta(t)$ is the BCS weak coupling energy gap. Lacy and Daniel employ the values $A_1 = 3.4$, $A_2 = 10$. This model gives an excellent fit to the data for $t > 0.7$ and it correctly predicts a maximum in Δ/kT_c. It fails to predict the low-temperature behavior, but the LD model applies to the limiting case $ql = 0$, while the 21-MHz data shown here have $ql\,(T=0) \simeq 0.8$. Hence the curve shown can be interpreted as a limiting case. Another feature of Fig. 5(a) is that the effective gap for high-frequency data tends toward essentially flat BCS behavior at low temperatures. Figure 5(b) is the zero-temperature gap implied by the effective gap values shown in Fig. 5(a). On this graph data independent of T/T_c would be characteristic of BCS behavior. Here again a frequency dependence is clearly visible with the low-temperatures higher-frequency data behavior more BCS-like. The frequency, as opposed to pure mean free path, dependence is also shown by comparing the work of Perz *et al.*[39] to the work of Levy *et al.*[40] in which the ultrasonically measured gap of high-purity tantalum behaves BCS-like for $ql = 10$ while low-frequency results show an effective gap with temperature dependence which is not BCS-like.

Figure 6 shows energy-gap analysis for shear waves at two frequencies. In Fig. 6(a) the effective energy gap is shown as in Fig. 5(a). In both plots of Fig. 6 there is a marked frequency dependence. The high-frequency data is BCS like for $0.18 < t < 0.48$ while the low-frequency data is nowhere so behaved. It is interesting that the high-frequency data displays a fairly abrupt change of form near $t = 0.5$. The domain $0.9 < t < 1$ is difficult to analyze. This is due to the fact that the earth's magnetic field causes a drop in the attenuation at $t = 0.9999$.

In order to better understand the domain $0.95 < t < 1$ which is erratic in Fig. 6, experimental data are presented in Fig. 7 which considers only the region near the transition. In Fig. 7(a) the drop in normalized attenuation at the transition is clearly visible. The drop for 51 MHz is slightly greater than that for 16.6 MHz. This additional drop could stem from the Meissner screening of the electromagnetic field set up by the lateral ionic motion.[10,41] The divergences observed in Fig. 7(b) for $t > 0.98$ are produced by the uncertainty in determining T_c in the earth's magnetic field.

In both Figs. 7(a) and 7(b) the frequency dependence of the superconducting attenuation is quite evident. This dependence has appeared regularly in the results presented here, and it is quite clearly a factor in the attenuation. This tends to support

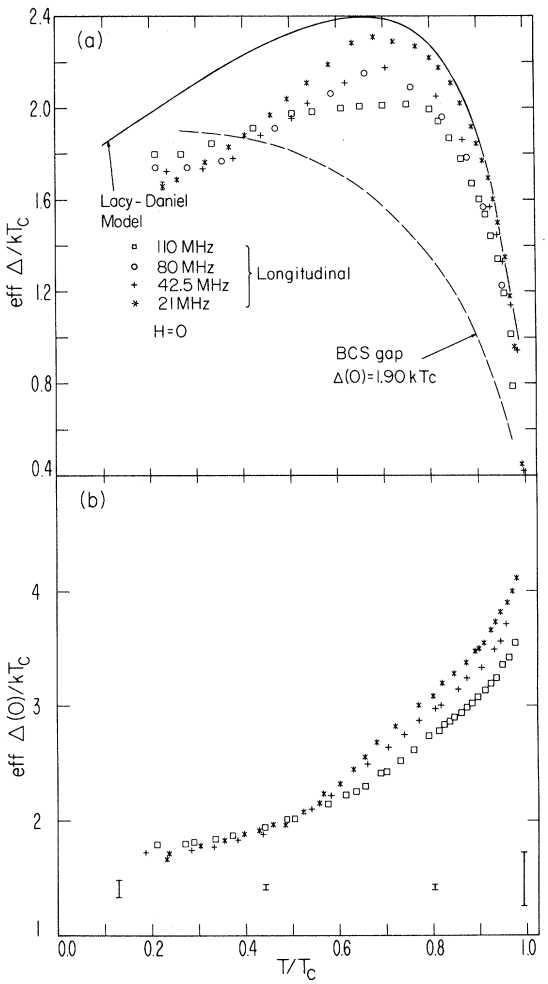

FIG. 5. Superconducting energy gap implied by longitudinal attenuation. (a) shows the energy gap evaluated according to BCS prediction $\alpha_s/\alpha_n = 2f(\Delta)$ while (b) shows the zero-temperature gap parameter $\Delta(0)$ predicted by each value of (a). In (a) the model of Lacy and Daniel is also shown. In (b) the 80-MHz data has been omitted for clarity—it was largely indistinguishable from 42.5-MHz results.

the approach of Fate–Trivisonno. On the other hand, the effective gap results of Figs. 5 and 6 are in good agreement with the model of Lacy and Daniel. Here the difficulty is that the low-temperature regime is the regime of poorest fit while this should be the very domain where the LD model is at its best since the two bands will contribute most independently and the s-band condensation will possess its largest gap.[27–29] It is clear that the FT and LD models are independent and noncontradictory as well as incomplete. It is also clear that both models are partly successful. What is needed is a rigorous model, such as was undertaken by Maki[1,19,20,22] and Tang,[30] which involves both the mean free path and the two-band hypothesis.

In Table I the results of our investigation are summarized. Energy-gap parameters are given for

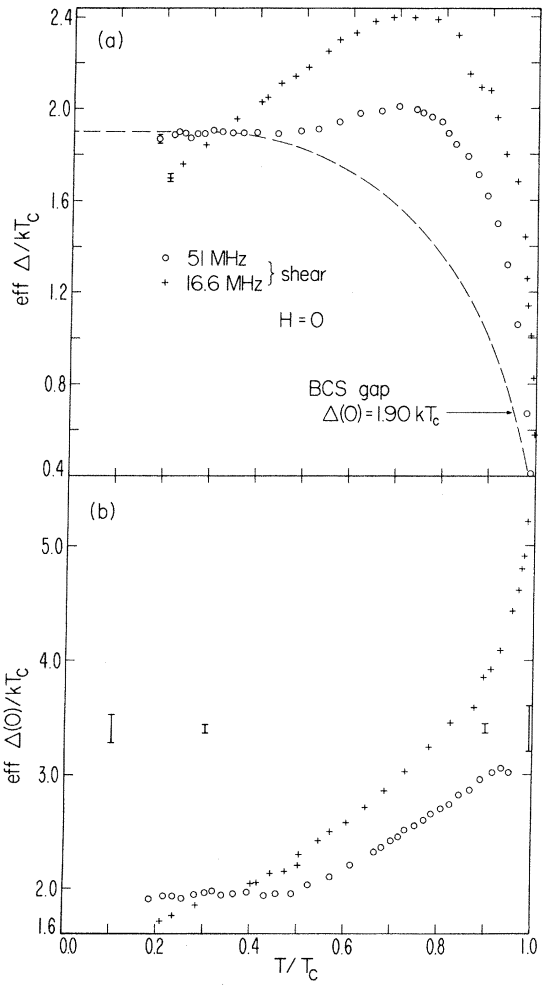

FIG. 6. Superconducting energy gap implied by shear attenuation. (a) shows the energy gap evalutated according to the BCS prediction $\alpha_s/\alpha_n = 2f(\Delta)$ while (b) shows the zero-temperature gap parameter $\Delta(0)$ predicted by each value of $\Delta(t)$ of (a).

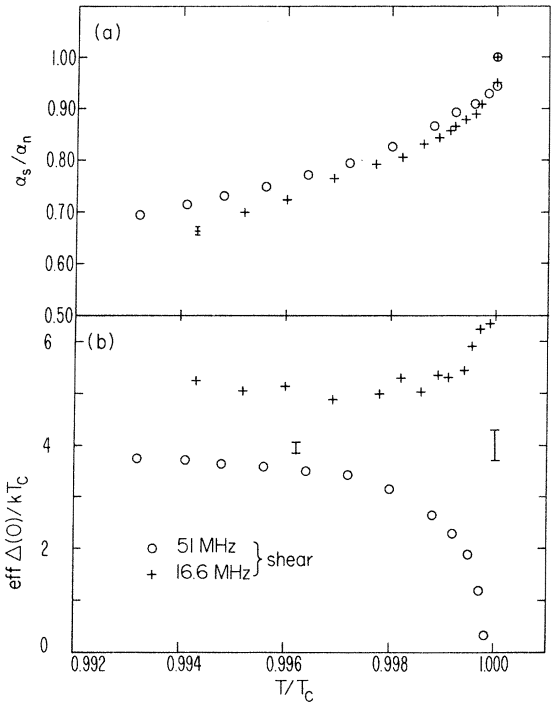

FIG. 7. Shear data near the zero-field transition. (a) shows the ratio α_s/α_n while (b) shows the zero-temperature gap parameter $\Delta(0)$ required to produce the values of α_s/α_n of (a). The BCS temperature dependence of Δ is assumed for each point.

the low-temperature limit, $\Delta_{BCS}(0)$. In conjunction with the model of Maki the function $f(x)$ and the parameter x are developed from both normal and superconducting data. In general the model of Maki is insufficient in predicting the deviation from BCS expectations. The low-temperature gap parameters, called $\Delta_{BCS}(0)$ here, are larger than those most often found[1,6,42,43] but are in good agreement with the tunneling work of MacVicar and Rose.[44]

In summary, we have measured the ultrasonic attenuation in the normal and superconducting state in pure niobium for both longitudinal and shear waves in the frequency domain 15–110 MHz and for $0.4 < ql < 0.6$. These data were compared with the models of Fate and Trivisonno, Lacy and Daniel, and Maki. Although the model of Fate and Trivisonno anticipates the frequency dependence obtained for the ratio α_s/α_n, it does not provide a temperature dependence for the ratio l_s/l_n which is needed in the evaluation of the energy gap. On the other hand, Maki does not consider the frequency dependence but does predict the value of the ratio l_s/l_n in addition to its temperature dependence. Maki's approach is partially successful in explaining the behavior of the attenuation in moderately pure samples, but appears to be inadequate for the high-purity samples reported here. The

interband coupling model of Lacy and Daniel accurately predicts a maximum in the temperature dependence of the effective energy gap as measured ultrasonically. This model does not contain frequency dependence for α_s/α_n as has been reported by many investigators, nor does it consider the mean-free-path dependence. Furthermore, the authors believe that in the absence of arguments to the contrary an interband coupling model should be most effective in the low-temperature regime rather than the regime of the transition. Clearly a vigorous approach such as that of Maki is called for in which interband coupling terms as well as mean-free-path and frequency effects are considered. Further experimental work should undertake a study of the region $ql \ll 1$ for long-mean-free-path samples and should attempt to outline the difference between the l dependence and ql dependence for ultrasonic attenuation in the superconducting state.

The authors wish to thank R. E. Reed for providing us with the high-purity niobium single crystal used during the course of this investigation. The authors are also indebted to J. Heiserman for his aid and to R. Williams, K. Maki, T. Holstein, and M. Harrison for their helpful discussions.

---

†Research sponsored by the Air Force Office of Scientific Research under AFOSR Grant No. 71-2079.

*Currently a Resident Research Associate of the National Academy of Sciences.

[1]F. Carsey, R. Kagiwada, M. Levy, and K. Maki, Phys. Rev. B **4**, 854 (1971).

[2]B. C. Deaton, Phys. Rev. **177**, 688 (1969).

[3]C. P. Newcombe and R. W. Shaw, Phys. Rev. **173**, 509 (1968).

[4]W. A. Fate and R. W. Shaw, Phys. Rev. Lett. **19**, 230 (1967); W. A. Fate, R. W. Shaw, and G. L. Salinger, Phys. Rev. **172**, 413 (1968).

[5]J. Trivisonno, J. Washick, M. J. Keck, and R. Reifenberger, J. Low Temp. Phys. **4**, 97 (1971).

[6]N. Tsuda and T. Suzuki, J. Phys. Chem. Solids **28**, 2487 (1967); and N. Tsuda, S. Koike, and T. Suzuki, Phys. Lett. **22**, 414 (1966).

[7]M. Levy, F. Carsey, and R. Kagiwada, in *Prodeedings of the Twelfth International Conference on Low-Temperature Physics*, edited by Eizo Kaude (Academic of Japan, Kyoto, 1971), p. 273.

[8]T. Tsuneto, Phys. Rev. **121**, 402 (1961).

[9]J. Bardeen, L. N. Cooper, and J. R. Schrieffer, Phys. Rev. **108**, 1175 (1957).

[10]M. Levy, Phys. Rev. **131**, 1497 (1963).

[11]J. C. Swihart, IBM J. Res. Dev. **6**, 14 (1962).

[12]Y. Wada, Rev. Mod. Phys. **36**, 253 (1964).

[13]I. Giaever, *Proceedings of the Eighth International Conference on Low-Temperature Physics, 1962*, edited by R. O. Davies (Butterworth, London, 1963), p. 188.

[14]J. Sutton and P. Townsend, in Ref. 13, p. 182.

[15]I. Dietrich, in Ref. 13, p. 173.

[16]L. L. Lacy and A. C. Daniel, Phys. Rev. Lett. **27**, 1128 (1971).

[17]F. Carsey, Ph.D. dissertation (UCLA, 1971) (unpublished).

[18]F. Carsey and M. Levy, Phys. Rev. Lett. **27**, 853 (1971).

[19]K. Maki, Prog. Theor. Phys. **41**, 586 (1969).

[20]K. Maki, Prog. Theor. Phys. **31**, 378 (1964).

[21]V. Ambegaokar and A. Griffin, Phys. Rev. A **137**, 1151 (1965).

[22]K. Maki, Phys. Kondens. Mater. **8**, 305 (1969).

[23]G. M. Eliashberg, Zh. Eksp. Teor. Fiz. **39**, 1437 (1969) [Sov. Phys.-JETP **12**, 1000 (1961)].

[24]A. B. Pippard, Philos. Mag. **46**, 1104 (1955); M. H. Cohen, M. J. Harrison, and W. A. Harrison, Phys. Rev. **117**, 937 (1960).

[25]J. W. Garland, Phys. Rev. Lett. **11**, 111 (1963).

[26]L. Y. L. Shen, N. M. Senozan, and N. E. Phillips, Phys. Rev. Lett. **14**, 1026 (1965).

[27]J. W. Hafstrom, R. M. Rose, and M. L. A. MacVicar, Phys. Lett. A **30**, 379 (1969).

[28]J. W. Hafstrom and M. L. A. MacVicar, Phys. Rev. B **2**, 4511 (1970).

[29]H. Suhl, B. T. Matthias, and L. R. Walker, Phys. Rev. Lett. **6**, 677 (1961).

[30]I-Ming Tang, Phys. Rev. **82**, 2581 (1970); Phys. Lett. A **31**, 480 (1970).

[31]A. C. Thorsen and T. G. Berlincourt, Phys. Rev. Lett. **1**, 244 (1961).

[32]D. A. Robinson, Ph.D. dissertation (UCLA,1971) (unpublished).

[33]R. C. MacFarlane, J. A. Rayne, and C. K. Jones, Phys. Lett. A **24**, 197 (1967).

[34]K. C. Hepfer and J. A. Rayne, Phys. Rev. B (to be published).

[35]M. Levy, R. Kagiwada, and I. Rudnick, Phys. Rev. **132**, 2039 (1963).

[36]J. A. Rayne and C. K. Jones, Phys. Acoustics **7**, 149 (1970).

[37]E. Fawcett, W. A. Reed, and R. R. Soden, Phys. Rev. 159, 533 (1967); W. A. Reed and R. R. Soden, *ibid.* 173, 677 (1968).

[38]R. A. Ferrell, Z. Phys. **182**, 1 (1964).

[39]J. M. Perz and W. A. Roger, Can. J. Phys. **49**, 296 (1971).

[40]M. Levy, F. Carsey, and R. Kagiwada, in Ref. 7, p. 273.

[41]L. T. Claiborne and R. W. Morse, Phys. Rev. **136**, 893 (1964).

[42]R. S. Kagiwada, Ph.D. dissertation (UCLA, 1966) (unpublished).

[43]J. M. Perz, J. Phys. C **3**, 438 (1970).

[44]M. L. A. MacVicar and R. M. Rose, J. Appl. Phys. **39**, 1721 (1968).